

Discovery and Characterization of Cross-Area and Intra-Area SSOs Sensitive to Delay in Droop Control of Grid-Forming Converters

Lilan Karunaratne, *Student Member, IEEE*, Nilanjan Ray Chaudhuri, *Senior Member, IEEE*,
Amirthagunaraj Yogarathnam, *Member, IEEE*, and Meng Yue, *Member, IEEE*

Abstract—Subsynchronous oscillations (SSOs) involving grid-forming converters (GFCs) are in a less familiar territory of power system dynamics. This letter reports a new phenomenon namely *cross-area* SSOs in grids with 100% droop-controlled GFC-based renewable penetration, which was discovered during our study on evaluating the adequacy of quasistationary phasor calculus (QPC) and space phasor calculus (SPC)-based models in capturing SSOs. We present frequency-domain characterization of such oscillatory modes in addition to intra-area SSOs in grids involving GFCs and study the impact of a delay in power-frequency droop feedback loop in regards to their stability. Electromagnetic transient (EMT) simulations validate our findings.

Index Terms—EMT, grid-forming converter, IBR, modeling adequacy, subsynchronous oscillations, SSO.

I. INTRODUCTION

Several incidents of subsynchronous oscillations (SSOs) involving grid-following converters (GFLCs) have been witnessed in bulk power systems in different parts of the world. Based on the root cause analysis, this phenomena can be divided into three categories - (a) series capacitor SSO [1], (b) weak grid SSO [1], and (c) inter-inverter-based resource (IBR) SSO [2]. Although papers including [1], [2] have explored SSO phenomena involving GFLCs, SSO involving grid-forming converters (GFCs) was only recently reported in [3] and in our work [4].

Inter-IBR SSO reported in [2] can be categorized as *intra-area* oscillations, i.e., IBRs in the same area oscillate against each other. On the other hand, [3] reported *inter-area* oscillations under 100% IBR penetration, where IBRs in different areas oscillate against each other. In essence, the oscillation groupings are characteristically similar to intra- and inter-area oscillations involving synchronous generators (SGs) [5].

In this letter, we report the discovery of a different type of oscillatory mode in the IEEE 2-area system [5] with SGs replaced by droop-controlled GFCs. In our case, unlike typical inter-area oscillations, the IBR groups are formed across the areas and each group oscillates against the other (see Fig. 3). Therefore, these oscillations can neither be categorized as intra- nor inter-area oscillations. We call this *cross-area* SSO.

This work is supported under Agreement 37532 by the Advanced Grid Modeling (AGM) Program of the Office of Electricity, the Department of Energy (DOE).

L. Karunaratne and N. R. Chaudhuri are with the School of Electrical Engineering and Computer Science, Penn State University, University Park, PA, USA e-mail: lvk5363@psu.edu, nuc88@psu.edu.

A. Yogarathnam and M. Yue are with the Interdisciplinary Science Department, Brookhaven National Laboratory, Upton, NY, USA e-mail: ayogarath@bnl.gov, yuemeng@bnl.gov.

In addition to the cross-area mode, we also observe intra-area SSOs in the IEEE 2-area system with 50% and 75% IBR penetrations. Frequency-domain characterization of such SSOs is performed and the impact of delay in the power-frequency droop control of GFCs towards the stability of these modes is assessed using space phasor calculus (SPC)-based models. The observations were validated using electromagnetic transient (EMT) models. We show that the quasistationary phasor calculus (QPC)-based models cannot capture the SSO modes.

II. MODELING IN SPC AND QPC FRAMEWORKS

Both SPC- and QPC-based models are built upon space phasors (also called space-vectors) denoted by $\bar{x}(t)$. The time-varying phasor $\bar{x}_{bb}(t)$ is calculated by the frequency shift operation on $\bar{x}(t)$ leading to $\bar{x}_{bb}(t) = x_d(t) + jx_q(t) = \bar{x}(t)e^{-j\rho(t)}$, where $\frac{d\rho(t)}{dt} = \omega(t)$. The operator $\tilde{Y} : \mathcal{M} \rightarrow \mathcal{D}$ is defined as $\bar{x}_{bb}(t) = \tilde{Y}(\mathbf{x}(t))$, where \mathcal{M} is a vector space representing the set of balanced three-phase signals. It can be shown that $\tilde{Y}(\mathbf{x}(t)) = [1 \ j \ 0]\mathcal{P}(t)\mathbf{x}(t)$, where $\mathcal{P}(t)$ is the Park's transformation matrix. As opposed to SPC, QPC-based models consider certain approximations in modeling some of the components as summarized in Table I. Dynamic models of SGs and GFCs are developed in respective rotating d - q frames, while the transmission network and loads are represented in a synchronously rotating D - Q frame. For more details, readers are referred to the previous works [4], [6] of the authors. Nonetheless, for the sake of completeness, the key aspects of GFC modeling and controls are concisely presented in the following subsection.

Table I
SUMMARY OF COMPONENT MODELING IN DIFFERENT FRAMEWORKS

Component	Modeling framework	
	QPC	SPC
SG stator transients	neglected	dynamically modeled
Transmission network	Y-bus	dynamically modeled
Loads	static load model	dynamic load model
GFC	identically modeled	

A. Modeling of GFC and its controls

A generic circuit diagram of a GFC is illustrated in Fig. 1(a). The notations used are self-explanatory and adhere to conventional meanings. The ac-side of the GFC is modeled and controlled in SPC framework that employs a rotating d - q frame whose angular frequency ω_c is determined by the power frequency droop mechanism depicted in Fig. 1(b).

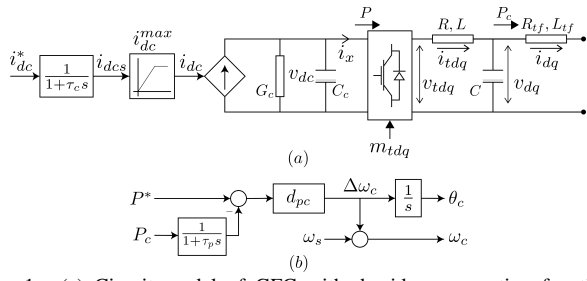


Figure 1. (a) Circuit model of GFC with dc-side representing functional model of a renewable source, (b) power-frequency droop with delay τ_p .

Additionally, the standard inner current and voltage control loops, and outer voltage control loop are employed to regulate ac-side quantities as shown in Fig. 2.

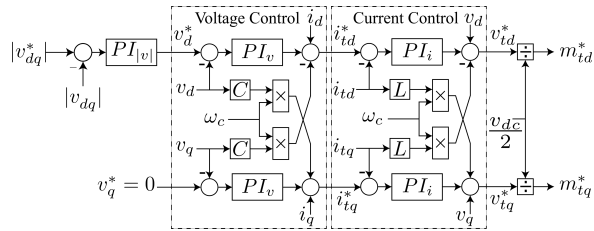


Figure 2. Inner current and voltage control loops, and outer voltage control loop of GFC.

III. CASE STUDIES

A. Test systems and modeling frameworks: In this section, we delve into characterization of the SSO modes involving GFCs using case studies performed on the IEEE 2-area 4-machine test system [5] modified by different IBR penetration levels after replacing some or all of the SGs by GFCs. Moreover, the impact of delay τ_p in power-frequency droop feedback loop (Fig. 1(b)) is studied to understand its influence on such modes. All test systems considered operate with approximately 400 MW tie-line flow. Our analysis will concentrate on four specific case studies: case (1): 50% IBR penetration replacing G1 and G4; case (2): 50% IBR penetration replacing G1 and G2; case (3): 75% IBR penetration replacing G1, G2, and G3; and case (4): 100% IBR penetration (see, Fig. 3). However, due to space constraints, we will discuss case (4) in details and findings from other cases are summarized.

To that end, QPC and SPC-based models of the test systems are developed in Matlab/Simulink [7]. EMT models of the same systems are built in EMTDC/PSCAD [8], where averaged models of the converters are considered along with distributed parameter representation of transmission lines, and (dynamic) constant impedance models of the loads.

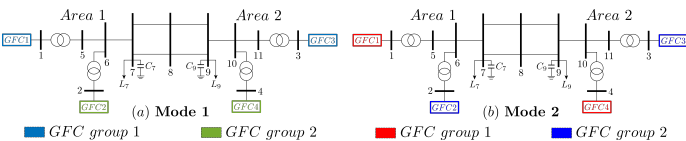


Figure 3. Case 4: *Cross-area* SSO modes forming distinct GFC groups in modified IEEE 2-area test system with 100% IBR penetration.

B. Modeling adequacy- SPC vs QPC: We perform the modeling adequacy study including frequency-domain analysis as

proposed in [6] on the linearized QPC and SPC-based models. For all cases, the QPC-based models cannot capture the SSO modes and are therefore deemed inadequate, whereas the SPC-based models can capture these modes. As an example, the maximum singular value (SV) plots of the 4-input-12-output linearized models based on QPC and SPC with $\tau_p = 2$ ms for case (4) are illustrated in Fig. 4(a), where a signal modulating active power references to the GFCs are inputs, and the dc-link voltages and transformer currents of the GFCs are outputs.

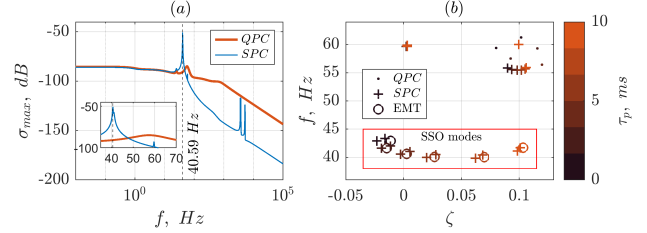


Figure 4. Case (4): (a) Comparison of maximum singular values of QPC and SPC models when $\tau_p = 2$ ms, (b) the loci of the SSO modes as the delay τ_p varies.

The SPC-based model exhibits a sharp peak in gain around 40.59 Hz representing an unstable mode with $\zeta = -0.27\%$ (Mode 2 in Fig. 3) as shown in Fig. 4(b), while the QPC-based model lacks this characteristic. Figure 4(b) indicates another SSO mode of 41.06 Hz with $\zeta = 0.55\%$ (Mode 1 in Fig. 3), which is stable and does not appear in the SV plot in Fig. 4(a). Both the SSO modes are absent in the QPC model (Fig. 4(b)). This observation is consistent with QPC and SPC-based models of rest of the cases, and indicates inadequacy of QPC models.

C. Characterization of SSO modes from SPC-based models: The SSO mode characterization is performed through frequency-domain analysis of all four cases. The results shown in this section assume $\tau_p = 2$ ms for SPC-based models.

(I) *Cross-area mode:* First, we focus on the characterization of the most interesting SSO modes, which we call *cross-area* modes. Figure 5 illustrates the compass plots of normalized participation factor magnitudes and modeshape angles of the dominant states contributing to these modes (highlighted in Fig. 4(b)). The most dominant states associated with the SSO modes are terminal and transformer currents of GFCs and current states of transmission line segments (i.e., $i_{DQ_{5-6}}$, $i_{DQ_{11-10}}$) that connect some of the GFCs to the network.

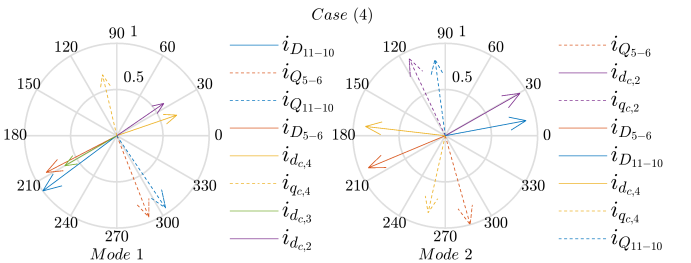


Figure 5. Case (4): Compass plots of normalized participation factor magnitudes and modeshape angles of the dominant states contributing to the *cross-area* SSO modes for $\tau_p = 2$ ms.

Unlike traditional *inter-area* modes, where groups of SGs or IBRs in one area oscillate against another group in an

electrically-distant area [3], [5], we observe a different characteristic in these modes. Here, two GFCs in different areas group together and oscillate against the remaining two GFCs across those areas, which we refer to as *cross-area modes*.

The modeshape angles relating to Mode 2 indicate that GFC1 and GFC4 as a group oscillate against GFC2 and GFC3, see Fig. 3(b). Conversely, the modeshape angles for Mode 1 suggest that GFC1 and GFC3 oscillate against GFC2 and GFC4 as shown in Fig. 3(a). Regardless of how the GFCs are grouped, an intriguing commonality is that the groupings consistently involve GFCs from two different areas – a phenomenon not observed before.

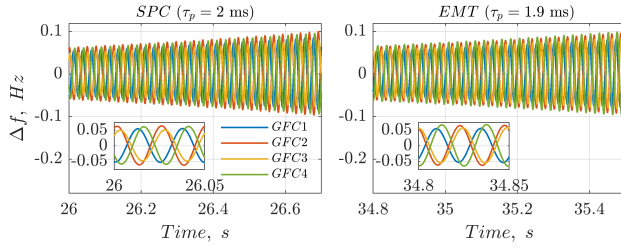


Figure 6. Case (4): Comparison of frequency dynamics of GFCs obtained from SPC and EMT simulations showing cross-area Mode 2.

Based on the singular value plot from the SPC model in Fig. 4(a), Mode 2 in this case is expected to dominate the dynamic behavior of the system. This fact is further verified by the time-domain responses of frequency dynamics from SPC and EMT simulations shown in Fig. 6, which also validate the GFC groupings in the cross-area Mode 2. For EMT simulation $\tau_p = 1.9$ ms was used, which corroborated with the SPC case with $\tau_p = 2$ ms. Prony analysis on the EMT model's responses reveals that the frequency of oscillation is 40.69 Hz with $\zeta = -0.24\%$, which is pretty close to what we observe for Mode 2 of the SPC model.

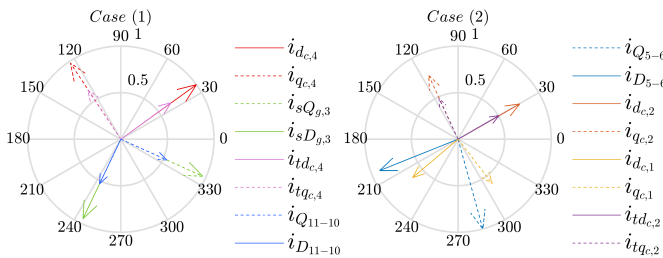


Figure 7. Case (1) and (2): Compass plots of normalized participation factor magnitudes and modeshape angles of the dominant states contributing to the *intra-area* SSO modes for $\tau_p = 2$ ms.

(II) *Intra-area mode*: For case (1) and case (2), the SSO modes observed can be categorized as *intra-area* modes, since in both cases, the machines involved belong to the same area (see Fig. 7). An important observation is that for case (1) when the GFC interacts with a SG within the same area, the resulting SSO mode remains stable. Conversely, for case (2) an interaction between two GFCs within the same area may lead to an unstable SSO mode for certain values of τ_p as shown in Table II. For case (3), two separate *intra-area* modes, one among GFC1 and GFC2 and the other among G3 and GFC4

are observed, where the former is unstable for certain τ_p values (Table II) and the latter is always stable (not shown in Table II). *D. Impact of delay (τ_p) on stability of SSO modes*: We found that the SSO modes are sensitive to the delay τ_p of the power feedback loop of the droop controller shown in Fig. 1(b). Figure 4(b) indicates the movement of SSO modes in case (4) as τ_p is varied from 0 to 10 ms. The results from EMT simulations are closely aligned with those of SPC model although only one of the modes is clearly observable in the EMT responses. Impact of delay for SSO modes of interest in cases (2) and (3) are shown in Table II. The modes become stable for all cases when delay becomes 3 ms or higher.

Table II
SSO MODE(S) OF INTEREST

Delay (τ_p), ms		0	1	2	3	5	10		
Case (2)	<i>intra-area mode</i>	EMT SPC	f, Hz	43.18	41.88	40.88	40.30	40.20	41.46
			$\zeta, \%$	-2.02	-1.58	0.08	2.32	6.46	9.89
		EMT SPC	f, Hz	43.13	41.90	40.94	40.35	40.17	41.38
			$\zeta, \%$	-1.33	-0.86	0.30	2.54	6.60	10.10
Case (3)	<i>intra-area mode</i>	EMT SPC	f, Hz	43.13	41.82	40.82	40.23	40.11	41.37
			$\zeta, \%$	-2.11	-1.69	-0.03	2.22	6.37	9.85
		EMT SPC	f, Hz	43.09	41.87	40.85	40.27	40.08	41.29
			$\zeta, \%$	-1.48	-0.98	0.22	2.45	6.50	10.03

IV. CONCLUSION

A detailed analysis was conducted using participation factors and mode shapes of the dominant states associated with SSO modes involving GFCs. This analysis revealed a new *cross-area* oscillatory mode, where GFCs from different areas group together and oscillate against the remaining GFCs. Specific to the IEEE 2-area system, the study further demonstrated that the SSO mode involving a GFC and SG from the same area remains stable. In contrast, interactions between two GFCs within the same area may result in an unstable SSO mode for this system. Moreover, the critical influence of a delay in the power-frequency droop feedback loop on the stability of SSO modes involving GFCs was examined. A delay of 3 ms was found to stabilize the unstable SSO modes in all the cases considered.

REFERENCES

- [1] Y. Cheng, L. Fan, J. Rose, S.-H. Huang, J. Schmall, X. Wang, X. Xie, J. Shair, J. R. Ramamurthy, N. Modi, C. Li, C. Wang, S. Shah, B. Pal, Z. Miao, A. Isaacs, J. Mahseredjian, and J. Zhou, "Real-world subsynchronous oscillation events in power grids with high penetrations of inverter-based resources," *IEEE Transactions on Power Systems*, vol. 38, no. 1, pp. 316–330, 2023.
- [2] L. Fan, "Inter-IBR oscillation modes," *IEEE Transactions on Power Systems*, vol. 37, no. 1, pp. 824–827, 2022.
- [3] M. Zhang, Z. Miao, L. Fan, and S. Shah, "Data-driven interarea oscillation analysis for a 100% IBR-penetrated power grid," *IEEE Open Access Journal of Power and Energy*, vol. 10, pp. 93–103, 2023.
- [4] L. Karunaratne, N. R. Chaudhuri, A. Yogarathnam, and M. Yue, "A case study on modeling adequacy of a grid with subsynchronous oscillations involving ibrs," 2024. [Online]. Available: <https://arxiv.org/abs/2407.09526>
- [5] P. Kundur, *Power System Stability and Control*. McGraw-Hill, 1994.
- [6] L. Karunaratne, N. R. Chaudhuri, A. Yogarathnam, and M. Yue, "An approach to evaluate modeling adequacy for small-signal stability analysis of IBR-related SSOs in multimachine systems," 2024 (under review). [Online]. Available: <https://doi.org/10.48550/arXiv.2403.07835>
- [7] *MATLAB version 9.10.0.2198249 (R2021a)*, The Mathworks, Inc., Natick, Massachusetts, 2021.
- [8] *PSCAD version 5.0.2.0(2023/04/14)*, Manitoba HVDC Research Centre, Winnipeg, Canada, 2023.